Faraday Discussions

Accepted Manuscript

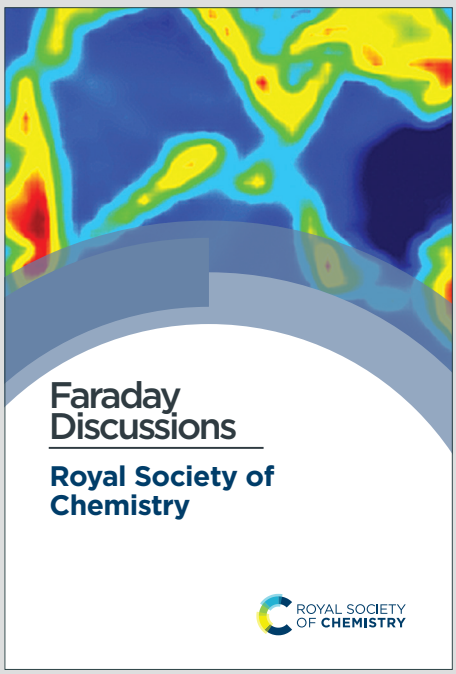

This article can be cited before page numbers have been issued, to do this please use: A. Freibert, S. Eckert, V. Vaz da Cruz, A. Föhlisch and N. Huse, *Faraday Discuss.*, 2026, DOI: 10.1039/D6FD00063K.

ROYAL SOCIETY OF CHEMISTRY

www.rsc.org/faraday_d

View Article Online
DOI: 10.1039/D6FD00063K

Understanding Resonant Inelastic X-ray Scattering Experiments of Diazines via Quantum Dynamics Simulation†

Antonia Freibert,*[a,b] Sebastian Eckert,[c] Vinícius Vaz da Cruz,[c] Alexander Föhlisch[c,d] and Nils Huse[b]

Received 00th January 20xx, Accepted 00th January 20xx DOI: 10.1039/x0xx00000x

We present a combined theoretical and experimental study of the three diazine isomers pyrazine, pyrimidine, and pyridazine by means of resonant inelastic X-ray scattering (RIXS) at the Nitrogen K-edge, employing fully time-dependent quantum dynamics simulations to understand the role of nuclear motion in core-excited states. The RIXS process is simulated by wavepacket propagation in both, the valence and core excited state manifold, carried out with the (multilayer) multiconfigurational time-dependent Hartree [(ML-)MCTDH] method. We use linear vibronic coupling Hamiltonians with up to 22 electronic states and compare a full-dimensional (24-mode) and a reduced six-mode model. We find good agreement between experiment and theory for all three molecules. In particular, our study highlights the essential role of nuclear motions during the population of short-lived intermediate core-excited states. Specifically, we show that ultrafast non-adiabatic transitions induce symmetry distortion that lead to additional emission bands, while interstate vibrational dynamics lead to vibrational progressions in the inelastic scattering spectra. These results establish a dynamical picture of the RIXS process in diazines that emphasises the importance of including nuclear dynamics in the calculations of resonant Raman processes.

Introduction

Diazines ($C_4N_2H_4$) are aromatic heterocyclic compounds containing two nitrogen atoms within a six-membered ring. They represent an important class of molecules in both fundamental research and applied sciences. The three structural isomers pyrazine, pyrimidine and pyridazine (see Figure 1) serve as model systems for investigating the influence of heteroatoms on aromaticity and electronic delocalisation as well as intramolecular relaxation dynamics.[1–9] In addition, diazines are key structural motifs in a wide range of applications, including pharmaceuticals,[10–13] agrochemicals,[14–16] functional materials,[17–19] and flavor and fragrance compounds.[20–22]

The photochemistry of diazines has been extensively investigated with a range of experimental and theoretical methods. Among the three isomers, pyrimidine and its derivates are the most intensively studied as pyrimidine constitutes the core structural framework of the nucleobases cytosine, thymine, and uracil and can therefore be regarded as a 'biological prototype'.[23–27] In contrast, pyridazine derivates rarely occur naturally and therefore have little biological role.[28] Nevertheless, it is of considerable interest in medicinal chemistry and drug design due to its distinctive physicochemical properties, including a high dipole moment, weak basicity, and dual hydrogen-bonding capacity. Diazines are associated with the α-effect, i.e. the enhanced susceptibility to nucleophilic attack arising at atomic sites adjacent to heteroatoms with lone pairs.[29–31] Pyrazine has become a benchmark system in the field of nonadiabatic dynamics due to its high symmetry and small molecular size, which make it computationally convenient while still exhibiting rich photophysical behavior. It has been shown that pyrazine displays efficient internal conversion between low-lying $n\pi^*$ and $\pi\pi^*$ states but despite extensive investigation using diverse non-adiabatic dynamics methods,[32–42] aspects of its detailed relaxation mechanisms remain under active debate.[43–49]

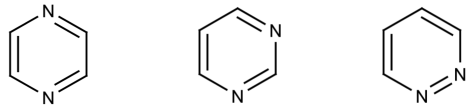

Figure 1 Lewis structures of pyrazine (1,4-diazabenzene), pyrimidine (1,3-diazabenzene) and pyridazine (1,2-diazabenzene).

Molecular spectroscopy provides a window into the electronic and nuclear structure of molecules by probing their interactions with electromagnetic radiation, yielding insights into chemical reactivity and functional behaviour. Among these techniques, X-ray spectroscopy is interesting for complex molecular systems because of its element specificity and chemical selectivity. Techniques such as X-ray absorption spectroscopy (XAS), X-ray photoelectron spectroscopy (XPS), Auger electron spectroscopy (AES), and resonant inelastic X-ray scattering (RIXS) offer complementary perspectives on occupied and unoccupied states, valence electronic structure, and electronic excitations. Of these techniques, RIXS has emerged as a versatile method capable of simultaneously probing core and valence electronic structure thereby accessing information on, for example, dissociation dynamics,[50,51] hydrogen-bond interactions,[52–55] proton transfer dynamics[56–60] or the photochemistry of transition-metal complexes.[61–68]

Conceptually, RIXS is a coherent Raman scattering process in which the system is resonantly excited into short-lived core-excited states, followed by spontaneous photon emission, returning the system to its electronic ground or energetically lower excited states.[69–71] This two-step scattering mechanism enables access to valence-excited states that may be symmetry-forbidden in linear absorption[72–74] and allows the investigation of low-energy excitations over a broad spectral range, even in condensed phases, without being limited by core-hole lifetime broadening.[75] Moreover, by adjusting the excitation energy RIXS allows controlling ultrafast core-excited state dynamics such as dissociation,[76,77] vibrational collapse,[78,79] or symmetry distortion.[80–82]

Harnessing the full capabilities of experimental techniques necessitates robust theoretical and computational modelling. Considerable efforts have therefore focused on the development of quantum chemical approaches based on both, wavefunction theory[83–93] and density functional theory,[94–96] to accurately describe core-excited states and simulate X-ray spectra. Both frameworks have demonstrated strong

View Article Online
DOI: 10.1039/D6FD00063K

performance in modeling linear and nonlinear X-ray spectroscopy.[97,98] An important aspect in simulations of nonlinear techniques as well as RIXS and AES is the treatment of nuclear motion and its impact on spectral observables.[99–104] Various strategies have been proposed to incorporate dynamical effects, ranging from frequency-domain formulations that account for interference effects via electronic-state superpositions,[72,105–107] to semiclassical methods suitable for larger systems,[108] and fully or partially time-dependent treatments within[57,109–111] and beyond the Born–Oppenheimer approximation.[112,113] Nevertheless, the multidimensional nature of excited-state potential energy surfaces (PESs) and the coupling among vibrational modes render X-ray–induced nuclear wavepacket dynamics highly complex, making the selection of the dominant driving modes not always straightforward.

In this work, we discuss different theoretical approaches for simulating X-ray spectroscopy and compare experimental RIXS spectra of all three diazine isomers recorded at the nitrogen K-edge with fully time-dependent simulations of both the X-ray absorption and RIXS spectra. The theoretical description is based on a full quantum-mechanical treatment of the electronic and nuclear degrees of freedom under symmetry-selective excitation conditions.[113] The simulations are performed within a diabatic representation of the Hamiltonian using the multiconfiguration time-dependent Hartree (MCTDH)[114] framework. We observe very good agreement between experimental measurements and theoretical predictions for all three molecules. The combined analysis highlights the impact of nuclear motion within the short-lived manifold of intermediate core-excited states. In particular, we demonstrate that ultrafast nonadiabatic transitions drive symmetry breaking in all three isomers, which gives rise to additional emission features in the RIXS spectra. Furthermore, interstate vibrational dynamics generate vibrational progressions in the inelastic scattering channels. By comparing reduced with full-dimensional models, we identify the dominant vibrational modes governing the RIXS process. This analysis describes the vibrational fine structure around the elastic peak with high precision and provides mechanistic insight into the interplay between electronic excitation and nuclear wavepacket dynamics.

Theoretical Framework

Quantum Mechanical Formulations of X-ray Spectroscopy

Under weak-field conditions, where time-dependent perturbation theory is applicable, spectroscopic observables can be generally formulated in two mathematically equivalent quantum-mechanical descriptions. In the energy-domain formulation, spectra are expressed through sums over stationary eigenstates of the system, while the time-domain representation uses appropriate time correlation functions. Spectral decomposition is the tool that allows to transform both representations into each other.

Assuming an intrinsic core-hole lifetime Γ_c for each element, which is reasonable for light elements where the lifetime is predominantly governed by Auger decay,[115,116] the linear X-ray absorption spectrum can be obtained by[117]

$$I_{\mathrm{XAS}}(\omega) \propto \sum_j |\langle \phi_j | \hat{\mu} | \phi_0 \rangle|^2 \cdot \frac{\Gamma_c/2}{(\tilde{\omega} - \omega_j)^2 + \Gamma_c^2/4} \tag{1}$$

commonly known as Fermi's golden rule. Here, $\hat{\mu}$ denotes the transition dipole moment operator, ϕ_j are excited state eigenstates with eigenenergy ω_j and $\tilde{\omega} = E_0 + \omega$ with E_0 being the eigenenergy of the initial eigenstate ϕ_0. Alternatively, the spectrum can be calculated in the time domain via the Fourier transform of the wavepacket autocorrelation function

$$I_{\mathrm{XAS}}(\omega) \propto \int_{-\infty}^{\infty} \mathrm{d}t \; C(t) e^{i\tilde{\omega}_I t - \Gamma_c t/2} \tag{2}$$

where $C(t) = \langle \Phi_0 | \Phi_0(t) \rangle$ is determined by $|\Phi_0\rangle \equiv \hat{\mu}|\phi_0\rangle$ and $|\Phi_0(t)\rangle = e^{-i\hat{H}_{\mathrm{mol}}t}|\Phi_0\rangle$ with the molecular Hamiltonian $\hat{H}_{\mathrm{mol}}$.

In particular, the energy-domain formulation (1) corresponds to a boundary-value problem which, for a single excitation energy, can be computationally advantageous compared to the time-dependent initial-value problem (2) where the time t appears as an additional variable. Nevertheless, the time-domain approach provides the entire absorption spectrum within a single calculation, since the time-dependent wavepacket encompasses all energies by *ansatz*. An additional advantage of the time-domain formulation, particularly in X-ray spectroscopy, arises from the presence of the phenomenological lifetime broadening. Owing to the finite core-hole lifetime, the propagation time required to obtain a numerically converged spectrum is typically limited to only a few femtoseconds and no additional convolution is required to smooth the spectrum, in contrast to *in silico* optical spectroscopy where artificial broadening is often introduced. However, since both formulations are formally equivalent, the question of which approach is more advantageous for numerical simulations and interpretation depends on the specific characteristics of the system under investigation and cannot be determined in a universally applicable manner.[118]

A similar correspondence exists for RIXS. The conventional way to calculate the RIXS cross section is given by

$$I_{\mathrm{RIXS}}(\omega_S; \omega_I) \propto \sum_f |\alpha_{f0}(\omega_I)|^2 \Delta(E_0 - E_f + \omega_I - \omega_S, \Gamma_f) \tag{3}$$

where the scattering polarisabilty tensor α_{f0} is defined by the well-known Kramers-Heisenberg-Dirac (KHD) formula[119–121]

$$\alpha_{f0}(\omega_I) = \sum_i \frac{\langle \phi_f | \hat{\mu}_S | \phi_i \rangle \langle \phi_i | \hat{\mu}_I | \phi_0 \rangle}{\tilde{\omega}_I - E_i + i\Gamma_c/2} \tag{4}$$

with $|\phi_0\rangle$, $|\phi_i\rangle$ and $|\phi_f\rangle$ being the initial, intermediate and final vibronic eigenstates involved in the resonance Raman process with energies E_0, E_i and E_f, respectively, and with a phenomenological Lorentzian line shape broadening

$$\Delta(\Omega, \Gamma) = \frac{\Gamma}{\pi(\Omega^2 + \Gamma^2)} \tag{5}$$

View Article Online
DOI: 10.1039/D6FD00063K

with full width at half maximum (fwhm) Γ. In particular, for RIXS the phenomenological broadening is independent of the core-hole lifetime. Moreover, ω_I and ω_S denote the incoming and outgoing photon frequencies, respectively, and Γ_f is the lifetime of the final excited states. The KHD equation involves a summation over all intermediate vibronic states of the molecule offering a static perspective of the Raman scattering event.

As for XAS, an equivalent time domain approach can be derived for RIXS where the spectrum is determined by [121]

$$I_{\mathrm{RIXS}}(\omega_S;\omega_I) \propto \int_{-\infty}^{\infty} \mathrm{d}t \; e^{-i\tilde{\omega}_S t - \Gamma_f t/2} \langle \tilde{\mathscr{R}}(\omega_I) | \tilde{\mathscr{R}}(\omega_I, t) \rangle \tag{6}$$

where $|\tilde{\mathscr{R}}(\omega_I,t)\rangle := e^{-i\hat{H}_{\mathrm{mol}}t}|\tilde{\mathscr{R}}(\omega_I)\rangle$ with $|\tilde{\mathscr{R}}(\omega_I)\rangle = \hat{\mu}_S|\mathscr{R}(\omega_I)\rangle$ is a wavepacket evolving in the final excited state manifold reached by the scattering event and

$$|\mathscr{R}(\omega_I)\rangle := \int_0^{\infty} \mathrm{d}\tau \; e^{-i(\hat{H}_{\mathrm{mol}} - i\frac{\Gamma_c}{2})\tau} \hat{\mu}_I e^{i\tilde{\omega}_I \tau} |\phi_i\rangle. \tag{7}$$

is the so-called Raman wavefunction, serving as an intermediate state that contains all dynamical information prior to the emission event.

To obtain an accurate description of the RIXS spectrum, the time-independent formulation based on the KHD expression requires knowledge of a large number of eigenstates on several PESs, as well as the proper treatment of interference effects. This approach becomes very quickly computationally demanding even for small molecular systems, and many practical implementations introduce approximations, e.g. neglecting interference terms, to remain tractable. Conversely, the time-dependent approach can exploit the limited probing of only a small region of the PESs and thus necessitates propagation over a brief time interval only while providing a high level of accuracy. Due to this reduced propagation time, the method can in principle yield numerically exact spectra. Moreover, the time-dependent approach provides a direct connection between the spectroscopic observables and the underlying nuclear dynamics. Since the present work is particularly concerned with the manifestation of ultrafast nuclear motion in the RIXS spectra of diazines, we employ the time-dependent formulations (2) and (6) to compute all spectral observables throughout this study unless otherwise explicitly stated.

Nuclear Quantum Dynamics and the Molecular Hamiltonian

To obtain the temporal evolution of the system, we perform nuclear quantum dynamics simulations using the MCTDH method [114,122,123] and its multilayer (ML-MCTDH) extension. [124–127] These approaches constitute grid-based, variational schemes for solving the time-dependent Schrödinger equation. Within the MCTDH framework, the high-dimensional nuclear wavefunction is represented as a sum of direct products of low-dimensional, time-dependent basis functions, which enables an efficient description of the system's time evolution. The ML-MCTDH formulation introduces a hierarchical tensor structure, providing a more efficient representation and enabling fully quantum-mechanical simulations of systems with up to several hundred degrees of freedom. Further methodological details can be found in the literature. [114,123,128,129]

A fully time-dependent description within the (ML-)MCTDH framework requires precomputed model Hamiltonians that accurately describe nuclear motion on both valence- and core-excited states. To construct such Hamiltonians, we adopt the strategy employed in earlier theoretical X-ray spectroscopic studies by some of the present authors. [113,130,131] In this approach, the full Hamiltonian is represented in a diabatic electronic basis and parametrised by a linear vibronic coupling (LVC) model for both the valence and core-excited states. The LVC model corresponds to a Taylor expansion of the electronic Hamiltonian around the ground-state equilibrium geometry and is conveniently expressed in terms of dimensionless, ground-state mass and frequency-scaled normal coordinates. Anharmonic effects can be incorporated by extending the LVC model with higher-order terms or additional diabatic functions. For a detailed account of the general theoretical framework, we again refer to the literature. [132–134] The specific Hamiltonian models employed in the present study are described in the Electronic Supporting Information (ESI).

Standard electronic structure calculations typically yield adiabatic electronic states that respect molecular symmetry and may therefore appear delocalised over equivalent atomic sites. However, core-excited states can be generally described in either a delocalised or a localised representation. In the delocalised picture core orbitals of symmetry-equivalent atoms form symmetry-adapted linear combinations that preserve the molecular point-group symmetry while the localised representation associates the core orbitals and corresponding excitations with individual atomic centres, providing a more intuitive description of site-specific excitation processes and local chemical environments. [135–138] Hence, core-excited states as obtained from electronic structure calculations can appear artificially distributed over several atoms, which may obscure the intrinsically local character of core excitations and complicate the interpretation of site-specific spectral features. For this reason, it is often advantageous in X-ray spectroscopy simulations to transform the symmetry-adapted adiabatic states into a localised diabatic representation, in which the core hole is associated with a specific atomic centre. This representation facilitates the interpretation of site-selective excitations and can simplify the treatment of vibronic coupling and symmetry breaking induced by nuclear motion. [82] However, it should be noted that, in general, localisation/delocalisation and diabatic/adiabatic describe different concepts: the former refers to the spatial distribution of electronic states, whereas the latter concerns the representation of the electronic Hamiltonian with respect to nuclear motion. While both pairs of representations are related by unitary transformations and thus formally equivalent, localised states are not generally identical to diabatic states and vice versa.

For all three diazine isomers, there are two energetically degenerate N 1s core orbitals that combine to form symmetry-adapted orbitals σ_{1s} and σ^*_{1s}, giving rise to two energetically degenerate N 1s $\rightarrow \pi^*$ core-excited electronic states. These states may interact through non-symmetrical vibrational normal modes, leading to vibronic coupling. [82,113] In a purely localised representation, both core-excited states are populated equally upon excitation, such that the effects of vibronic coupling are effectively incorporated implicitly. In the present work, we employ a diabatic Hamiltonian constructed from delocalised adiabatic electronic energies to explicitly describe vibronic coupling upon

View Article Online
DOI: 10.1039/D6FD00063K

core-excitation in these highly symmetric systems and to investigate its role in driving dynamical core-hole localisation and associated symmetry breaking. In this representation, only one of the two core-excitations is dipole-allowed from the ground state due to symmetry requirements, while the second excitation is dipole-forbidden. Vibronic coupling dynamically mixes the two core-excited states, allowing population transfer into the initially dark state and thereby enabling dynamical localisation of the core hole.[136]

Methodology

Experimental Details

The aqueous diazine solutions were prepared at a concentration of 0.5M. The pH was adjusted to ∼10 using sodium-hyroxide. The samples were injected into the sample-chamber of the EDAX-instrument at the beamline UE49_SGM[139] of the BESSY II electron storage ring, operated by the Helmholtz-Zentrum Berlin für Materialien und Energie, using a liquid jet with a diameter of 20 to 30μm. Details of the instrument can be found elsewhere.[140] In short, the solution was excited using horizontally polarized radiation at photon energies at the nitrogen K-edge of around 400eV and a bandwidth of ∼200meV. The emitted radiation was detected in a 90° scattering geometry using the 1200 l/mm grating and a position sensitive MCP detector of a modified Scienta XES 350 spectrometer. The presented absorption spectra are partial fluorescence yield measurements integrating the nitrogen K-edge emission signal in the RIXS spectra as a function of the exciting photon energy. Supporting measurements were performed at the instrument NEXAFS@UE52_SGM.[141]

Computational Details

The diabatic molecular Hamiltonian of pyrazine was adopted from previous studies[131]. To parametrise the Hamiltonians of pyrimidine and pyridazine, ground-state geometry optimisations and harmonic frequency calculations were performed using the second order Møller-Plesset (MP2) theory[142] with the Dunning correlation consistent basis set cc-pVDZ,[143] as implemented in the Gaussian 16 software package.[144] Valence-excited-state properties were computed using the equation-of-motion coupled cluster singles and doubles (EOM-CCSD) method,[145] while core-excited-state properties were obtained employing the frozen-core core–valence-separation (fc-CVS-) EOM-CCSD approach.[90] In all cases, Dunning's correlation consistent basis set aug-cc-pvDZ were employed, consistent with those used in our previous studies on pyrazine.[113,131] All excited-state electronic-structure calculations were carried out using the Q-Chem quantum chemistry package.[146]

The coupling parameters entering the linear vibronic coupling Hamiltonian were determined by minimising the root-mean-square deviation between the model energies and ab initio single-point energies computed at multiple nuclear configurations. To account for anharmonicity, selected vibrational modes were fitted using Morse or quartic potentials. The complete fitting procedure was performed using the VCHam programs as implemented in the Heidelberg MCTDH package.[147] A complete list of parameters for the full molecular Hamiltonian of pyrazine is provided in refs.[113] and[131], while the corresponding data for pyrimidine and pyridazine are given in the ESI.

Nuclear dynamics simulations were carried out using the (ML-)MCTDH method as implemented in the Heidelberg MCTDH package. For pyrazine, the mode-combination scheme, number of single-particle functions (SPFs), and grid parameters were adopted directly from ref.[113] without modification. The corresponding computational details for pyrimidine and pyridazine are reported in the ESI. Quantum dynamical propagations on the core-excited states were performed for at least 40 fs, covering more than 99 % of the decay associated with the 8 fs core-hole lifetime, which corresponds to a Lorentzian line width of 110 meV.[148] Propagations in the valence-excited states were carried out for 120 fs, with wavefunction data recorded every 0.25 fs, ensuring sufficient temporal resolution and frequency range for subsequent Fourier transform analyses.

Results and Discussion

X-ray Absorption Spectroscopy

In the present work, we focus on RIXS after excitations of core electrons from the N 1s orbitals to the lowest π^* resonance of diazines. For each isomer, the corresponding experimental and calculated absorption band is shown in Figure 2 together with the core excited state population dynamics following an instantaneous vertical excitation at time $t = 0$ fs and using a full dimensional model, i.e. including all 24 vibrational normal modes. In all cases, this absorption band is energetically well separated from the onset of the continuum absorption, as shown in the ESI. Notably, the absorption band associated with the lowest π^* resonance exhibits a systematic shift to higher energies, appearing at 398.4 eV, 398.6 eV and 399.0 eV for pyrazine, pyrimidine and pyridazine, respectively. We attribute this trend to the increasing interaction of the two nitrogen atoms' lone-pair charge densities, from the largest separation in pyrazine to direct neighbours in pyridazine. These lone-pair charge densities enhance the susceptibility of diazines to nucleophilic addition (α-effect)[149], and their direct proximity is advantageous for molecular recognition by the formation of two hydrogen bonds.[31]

For all three diazines, the simulated absorption band obtained by including only the intrinsic core-hole lifetime broadening (solid red line) is significantly narrower than the experimental spectrum (black line). However, after applying an additional Gaussian broadening (dashed red line) with Gaussian width parameter σ of 0.25 eV, 0.27 eV and 0.27 eV for pyrazine, pyrimidine and pyridazine, respectively, the overall shape of the lowest X-ray absorption band is reproduced well. Several factors may contribute to this additional broadening required to reconcile theory and experiment. Firstly, the simulated spectra are computed for isolated molecules at zero temperature, whereas the experiments were performed in aqueous solution at ambient temperature. Consequently, solvent-induced inhomogeneous broadening, arising from hydrogen bonding and other solute–solvent interactions, leads to increased spectral inhomogeneity. However, a previous study on pyrimidine by some of the present authors demonstrated that while the solvent environment indeed contributes to additional inhomogeneous broadening of the π^* absorption resonance, it does not fully account for the observed line width.[82] Secondly, the experimental absorption profiles are also broadened by thermal conformational distributions and the instrumental response function with an incident energy bandwidth of 200 meV fwhm.

For each isomer, a second, less intense X-ray absorption band is observed in the experimental spectrum, which can be attributed to higher-lying core-excited states. These states are not included in the present study, as they are not expected to induce significant changes

View Article Online
DOI: 10.1039/D6FD00063K

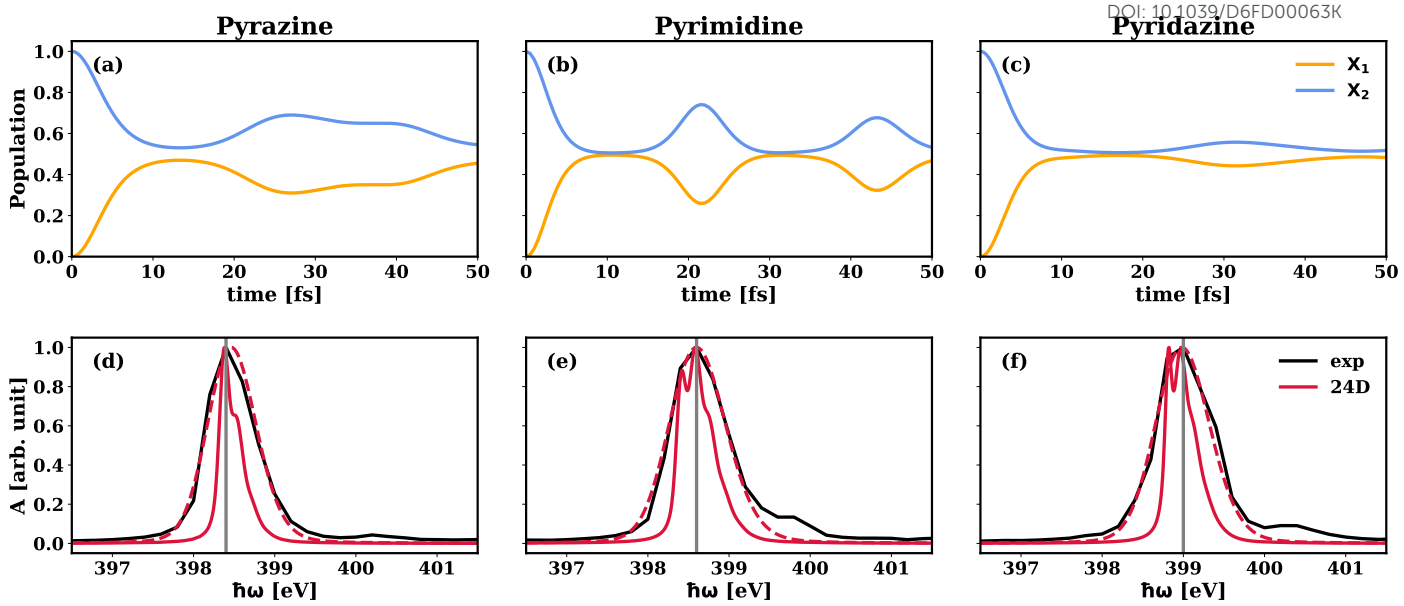

Figure 2 Top row: Normalised population dynamics of the core-excited diabatic states X_1 (orange) and X_2 (blue), following excitation to X_2 at the Franck–Condon point for (a) pyrazine, (b) pyrimidine, and (c) pyridazine. Bottom row: Experimental (black) and computed (red) static nitrogen K-edge X-ray absorption spectra of (d) pyrazine, (e) pyrimidine and (f) pyridazine. The solid red curves correspond to spectra obtained from quantum dynamical simulations including a core-hole lifetime of 8 fs without additional broadening. The dashed red curves show spectra with an additional Gaussian broadening applied. To align with the experimental spectra, rigid energy shifts of 3.82 eV, 3.95 eV, and 3.70 eV were applied to the calculated spectra of pyrazine, pyrimidine, and pyridazine, respectively. The vertical gray line indicates the excitation energy corresponding to zero detuning.

in the RIXS spectra because their transition dipole moments are considerably weaker than that of the lowest-lying π^* resonance. The following discussion therefore refers only to the respective lowest, significantly more intense absorption band.

Due to the presence of the two equivalent nitrogen atoms in the equilibrium ground-state structures, two energetically degenerate core excited states, denoted X_1 and X_2, arise for each isomer that correspond to transitions from the nitrogen 1s core orbitals into π^* valence orbitals. In the delocalised representation, the two degenerate nitrogen 1s orbitals combine linearly yielding symmetric and antisymmetric core orbitals, σ_{1s} and σ^*_{1s}, respectively. Under these symmetry constraints, there is only one dipole-allowed transition, namely, to the X_2 state, while the X_1 state remains dark. However, the two core-excited states are vibronically coupled through non-totally symmetric vibrational modes of b_{1u} symmetry in pyrazine and b_2 symmetry in pyrimidine and pyridazine. This coupling enables non-radiative population transfer between these two states and is responsible for symmetry breaking of the systems.[82,113] This coupling is reflected in the evolution of the normalised core-excited state populations shown in Figure 2. For each isomer, only the bright X_2 state is initially excited. Subsequently, a rapid population transfer to the dark X_1 state is observed, leading to a nearly equal population distribution within approximately 10 fs. The population dynamics exhibit oscillatory behaviour, with periods of about 30 fs, 20 fs, and 30 fs for pyrazine, pyrimidine, and pyridazine, respectively. These oscillations reflect the vibrational frequencies of the dominant coupling modes that mediate the interaction between the core-excited states. Detailed information on coupling parameters, vibrational frequencies, state characterisations, and molecular orbitals is provided in the ESI.

Resonant Inelastic X-ray Scattering

While the different broadening mechanisms in solution-phase XAS mask vibrational progressions and vibronic side-bands which reflect the system's dynamics, the RIXS spectra are known to be sensitive to the evolution of the nuclear wave packet in the core-excited state manifold. The sensitivity to nuclear motion mainly depends on the topology of the PESs involved and the coupling between them. However, the nuclear core-excited state dynamics can be limited by controlling the effective scattering duration[69,150]

$$T = \frac{1}{\sqrt{\Omega^2 + \Gamma_c^2}} \tag{8}$$

through variation of the amount of detuning Ω from the resonant excitation energy. In particular, excitations far from resonance allow to almost completely suppress dynamics during population of intermediate core-excited states. Importantly, the core-hole lifetime Γ_c controls the effective scattering time T but it does not fundamentally limit the final spectral resolution of RIXS measurements.

Figure 3 shows the RIXS spectra in an energy loss range up to 9 eV of the three diazines for different values of the detuning Ω. Here, $\Omega = 0$ eV denotes excitation energies of 398.4 eV for pyrazine, 398.6 eV for pyrimidine, and 399.0 eV for pyridazine, as marked by the vertical grey line in the XAS spectra in Figure 2. Both experimental (black line) and theoretical (red line) spectra were normalised to the elastic peak at zero energy loss. To better match the experiment, the theoretical elastic peaks were scaled to 40 %, 50 % and 50 % for pyrazine, pyrimidine, and pyridazine, respectively. This reduction of the experimentally measured elastic peak intensity can be attributed to the optical transfer function of the emission spectrometer and to self-absorption of the sample. Both aspects are not included in our theoretical models.

View Article Online
DOI: 10.1039/D6FD00063K

As described above, the dynamics involves two nearly degenerate core-excited states, namely a bright state, X_2, and a dark state, X_1, that are vibronically coupled, thereby enabling non-adiabatic population transfer between each other. To differentiate emission bands associated with either X_1 or X_2 as the intermediate state, the theoretical spectra are separated into two contributions where blue denotes transitions originating from the initially excited bright X_2 state while yellow indicates transitions originating from the dark X_1 state, which is exclusively populated via population transfer from X_2.

For each isomer the RIXS spectra obtained under off-resonant excitation conditions, e.g. with $\Omega = -0.6$ eV, exhibit no significant contribution from the dipole-forbidden X_1 state as an intermediate state. In this regime, the effective scattering duration, T, is already too short to allow non-adiabatic transitions to occur. Consistent with this interpretation, the elastic peak exhibits a clear Lorentzian profile and no resolved vibrational progression in any of the loss spectra, further demonstrating that the nuclear wavepacket does not evolve significantly off resonance.

In the inelastic region of the RIXS spectra with $\Omega = -0.6$ eV or lower, pyrazine exhibits a distinct emission band, whereas pyrimidine and pyridazine show rather broad features with two maxima, arising from a total of six and five emission channels, respectively. Moreover, the overall spectral profile remains essentially unchanged at larger negative detuning, further indicating that the effective scattering duration is negligible on the timescale of nuclear dynamics.

In contrast, for increasingly resonant excitation conditions ($\Omega \geq -0.4$ eV), the overall shape of the RIXS spectra changes significantly for the three diazines. In particular, emissive contributions from the initially dark X_1 state can be observed. Because the non-adiabatic coupling between core-excited states is mediated by non-totally symmetric normal modes which break the symmetry, the equivalence of the two nitrogen atoms is lifted. The resulting distinction between the two sets of scattering pathways therefore provides clear evidence of nuclear motion in the core-excited manifold and the associated dynamical localisation of the core hole. Since X_1 and X_2 possess different electronic state symmetries, the conventional quadrupole selection rules for Raman excitation are no longer strictly applicable,

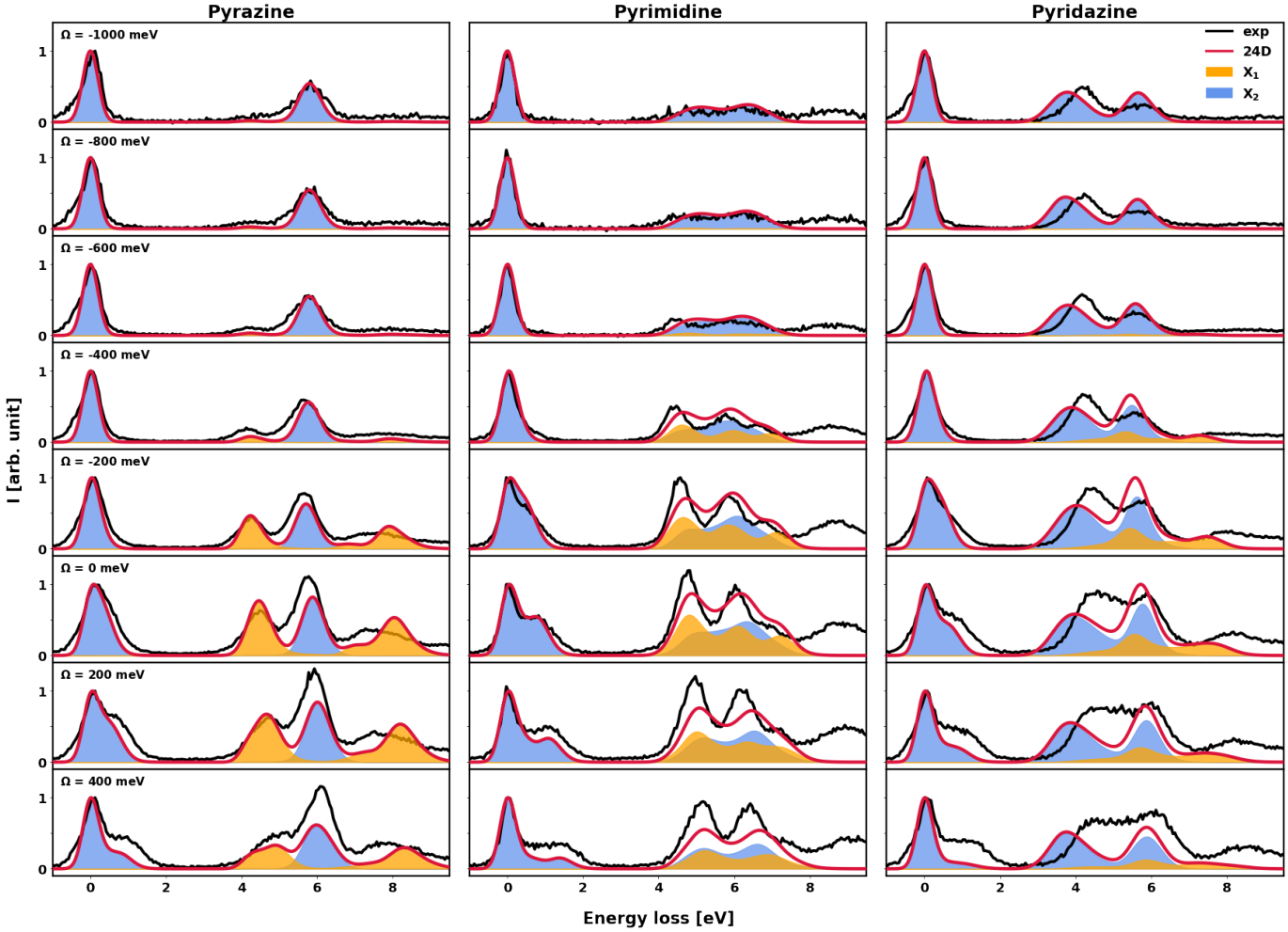

Figure 3 Experimental (black) and simulated (red) RIXS spectra for various amounts of detuning where $\Omega = 0$ eV is based on the experimental XAS as indicated by the vertical gray line in Figure 2. For a higher synergy between experiment and theory the theoretical incoming excitation energies were consistently shifted by 0.1 eV for pyrazine and 0.2 eV for pyrimidine and pyridazine. All spectra are independently normalised to their respective elastic peak height before rescaling the low energy loss region. The contributions of the transitions from X_1 and X_2 are highlighted in yellow and blue, respectively. When performing the Fourier transform a damping time of 80 fs was assumed and an additional Gaussian broadening was applied to match the experimental broadening of the elastic peak for far off resonant excitations.

View Article Online
DOI: 10.1039/D6FD00063K

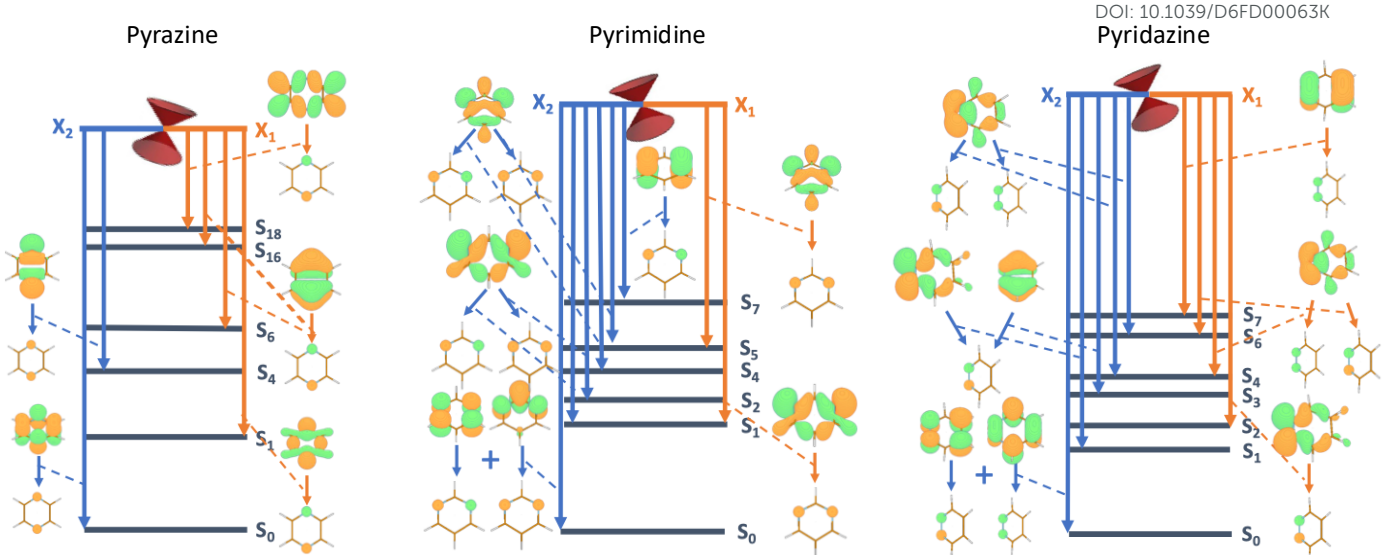

Figure 4 Schematic diagram of electronic transitions involved in the RIXS process of pyrazine, pyrimidine and pyridazine within this study. For each transition, the corresponding natural transition orbitals are shown in order to characterise the nature of the electronic excitation. The associated vertical excitation energies with respect to the S_0 energy at the ground-state equilibrium geometry and averaged transition dipole moments are reported in the ESI.

and electronic transitions that would remain forbidden for the symmetric molecule become allowed upon resonant excitation.

This effect is particularly pronounced in pyrazine where additional side bands appear in the inelastic region for (quasi-)resonant excitations. These spectral features can be assigned to four additional electronic excitations that originate from X_1 populations and are spectrally well separated from the inelastic emission band at approximately 6 eV energy loss that is associated with X_2 excitations. In contrast, for pyrimidine and pyridazine the contributions from X_1 and X_2 scattering pathways strongly overlap, making them much less distinguishable. The reason for the well separated energy loss bands in pyrazine compared to the other two diazines lies in its higher molecular symmetry. In the equilibrium ground-state structure, pyrazine belongs to the D_{2h} point group, whereas pyrimidine and pyridazine are characterised by C_{2v} symmetry. Pyrazine therefore obeys additional parity selection rules that do not apply to the other two diazines because they lack inversion symmetry. In particular, X_1 and X_2 in pyrazine have different parity imposed by the symmetry of the core orbitals, and transitions from these states into the same valence-excited final states are dipole forbidden, resulting in a stronger separation of emission features. In pyrimidine and pyridazine, by contrast, the absence of parity selection rules permits transitions from X_1 and X_2 into the same valence-excited states, resulting in significant spectral overlap of emission signals.

Figure 4 presents a schematic diagram of the RIXS process, highlighting the electronic character of each transition. While Figure 4 only includes the electronic states directly involved in the RIXS process, additional electronic states may become populated through non-adiabatic transitions and therefore also need to be included in the Hamiltonian. As a result, the Hamiltonians include the ground state and two core-excited states for each isomer, as well as the lowest 19 valence-excited states for pyrazine and the lowest 8 valence-excited states for pyrimidine and pyridazine covering the low-energy-loss region of the RIXS spectra, which display the most strongly influence by dynamical effects. Further details such as the averaged values of the corresponding transition dipole moments and vertical excitation energies can be found in the ESI.

Further motional effects are observed at the elastic peak for all three diazines. For resonant excitations, a pronounced shoulder emerges that can be attributed to vibrational progressions stemming from the inter- and intrastate core-excited state coupling. The loss spectra of valence excitations depend on dynamics in the core-excited and valence-excited states, making the selection of an appropriate reduced-mode model very challenging. However, the vibrational structure at the elastic peaks can be modelled well by considering only the dynamics in the core-excited states (omitting coupling among vibrational modes).

To better understand the contributions to the loss spectra around the elastic peak, we also employed a reduced model that includes only six vibrational normal modes, which primarily drive the core-excited state dynamics. The calculated elastic peak and the corresponding energy eigenstates, obtained by a Lanczos diagonalisation of the Hamiltonian, are shown in Figure 5. For the three molecules, the pronounced shoulder of the elastic peak that emerges under resonant excitation can be attributed to combined contributions of several vibrational normal modes. These modes generate vibrational progressions with different energy spacings, collectively giving rise to the broad-shouldered feature. Our calculations indicate that identification of these progressions even at RIXS spectrometers with very high-resolution ($\lesssim 20$ meV) may be difficult due to the dense overlap of multiple vibrational progressions. At zero detuning, however, distinct vibrational features remain identifiable such as the prominent lines at 0.2 eV for pyrazine and for pyrimidine, and the two lines at 0.18 eV and 0.20 eV for pyridazine. These energies are consistent with the harmonic frequencies of totally symmetric normal modes in the respective molecules, namely ν_{20} for pyrazine, ν_{19} for pyrimidine, and ν_{18} and ν_{19} for pyridazine. A table with all harmonic frequencies can be found in the ESI. These results demonstrate that an accurate description of RIXS requires accounting not only for non-adiabatic interstate coupling, which induces symmetry breaking, but also for intrastate vibronic coupling within the same core-excited electronic state that drives vibrational relaxation and is manifested primarily in the vibrational progression of the elastic peak.

View Article Online
DOI: 10.1039/D6FD00063K

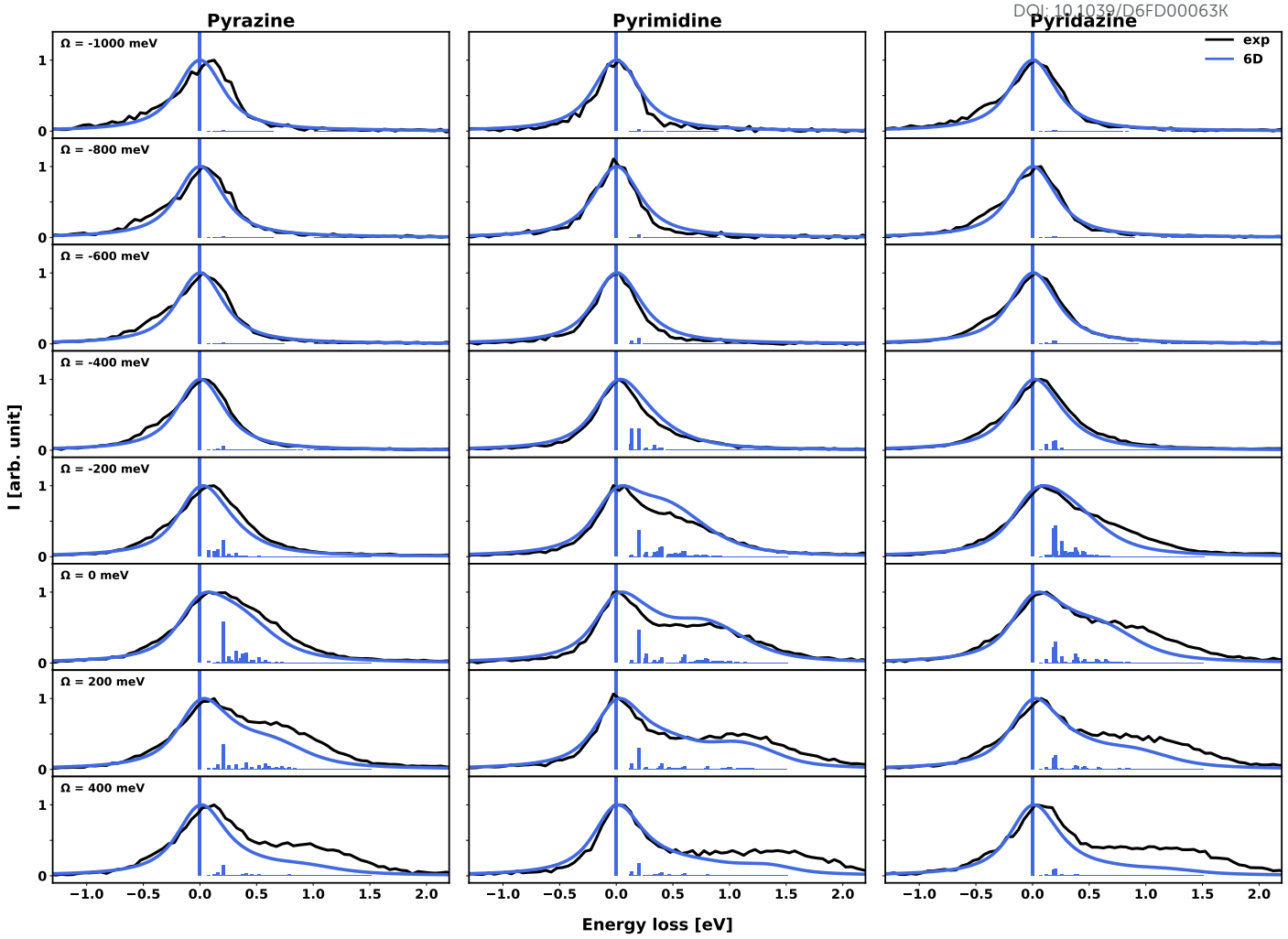

Figure 5 Experimental (black) and calculated (blue) elastic peak of the three diazines for the indicated energy detuning. These calculations were performed with reduced model Hamiltonians which include the six vibrational normal modes that mainly drive the core-excited state dynamics. The stick spectra were obtained from direct Lanczos diagonalisation in 2000 steps. The shape of the elastic peak and the vibrational progressions is obtained by a convolution of the sticks with a Voigt line-shape (Gaussian width parameter $\sigma = 0.2$ eV, Lorentzian width parameter $\alpha = 0.1$ eV.). For a better visibility, the stick intensities are rescaled by a factor of 2.

In summary, Figures 2-5 show very good agreement between experiment and theory, with all experimentally measured features reproduced and assigned to specific dynamical effects. Nevertheless, some discrepancies remain, which we attribute primarily to the essential difference between experiment and model, namely the treatment of an isolated molecule in the gas phase at 0 K in the calculations versus measurements performed in solution just below room temperature. Additional deviations may also arise from limitations of the theoretical model, including the chosen level of electronic structure theory, the basis set size, and the restriction to linear coupling terms in the Hamiltonian. Moreover, we find that the substantial broadening of the XAS spectrum arises from several contributions like instrumental limitations or solvent interactions which include hydrogen bonding that result in conformational effects. However, incorporating inhomogeneous broadening into the calculations of RIXS spectra is not straightforward. Specifically, the calculated RIXS spectra are based on a model Hamiltonian that includes only the intrinsic core-hole lifetime broadening and no additional broadening mechanisms. Consequently, a narrower absorption line-shape is modelled which is plotted as the solid line in Figure 2 which implies that discrepancies are already present for the excitation energies. For instance, significant absorption is still observed experimentally at -0.5 eV detuning for each isomer, but the calculations predict ten-fold less absorption at this energy detuning. This difference may also be the reason why an additional small excitation energy shift of 0.1 eV for pyrazine and 0.2 eV for pyrimidine and pyridazine is required for best agreement between theory and experiment.

Conclusions

In this work, we developed full- and reduced-dimensional model Hamiltonians comprising up to 22 electronic states for a more detailed understanding of the dynamical aspects in experimental RIXS at the nitrogen K-edge of diazines. All spectral properties were calculated within the time-dependent framework using the fully quantum-mechanical MCTDH approach. The good agreement between the experimental spectra and the quantum-dynamical simulations following vibronic excitation supports the validity of the simplified model

View Article Online
DOI: 10.1039/D6FD00063K

Hamiltonians. In particular, the simulations allow us to identify dynamical effects driven by several vibrational normal modes, including both interstate and intrastate coupling effects. These results underscore the importance of including a sufficiently large number of nuclear degrees of freedom for an accurate description of the RIXS process in these systems. Furthermore, the lower-dimensional models enable a vibrationally resolved description of the elastic peak for the studied cases.

Acknowledgements

A.Fr. and N.H. acknowledge financial support from the Cluster of Excellence 'CUI: Advanced Imaging of Matter' of the Deutsche Forschungs-gemeinschaft (DFG) – EXC 2056 – project ID 390715994. A.Fr. also acknowledge funding by the Deutsche Forschungsgemeinschaft (DFG, German Research Foundation) - TRR 352 - Project-ID 470903074 and by the TUM Laura Bassi Scholarship. We thank the Helmholtz-Zentrum Berlin für Materialien und Energie for the allocation of synchroton radiation beamtime. We also thank Jessica Harich for support in preparation of the beamtime.

Data availability

The data supporting this article have been included as part of the Supplementary Information.

Conflicts of interest

There are no conflicts to declare.

Notes and references

[1] H. Baba, L. Goodman and P. C. Valenti, *Journal of the American Chemical Society*, 1966, **88**, 5410–5415.

[2] I. Yamazaki, T. Murao, T. Yamanaka and K. Yoshihara, *Faraday Discuss. Chem. Soc.*, 1983, **75**, 395–405.

[3] G. Vall-llosera, B. Gao, A. Kivimäki, M. Coreno, J. Álvarez Ruiz, M. de Simone, H. Ågren and E. Rachlew, *The Journal of Chemical Physics*, 2008, **128**, 044316.

[4] Y. Wang, J. I.-C. Wu, Q. Li and P. v. R. Schleyer, *Organic Letters*, 2010, **12**, 4824–4827.

[5] C. P. Frizzo and M. A. P. Martins, *Structural Chemistry*, 2012, **23**, 375–380.

[6] K. A. Rinderspacher, *Progress in Heterocyclic Chemistry*, Elsevier, 2014, vol. 26, pp. 395–447.

[7] F. Feixas, E. Matito, J. Poater and M. Solà, *Chem. Soc. Rev.*, 2015, **44**, 6434–6451.

[8] S. K. Pandey, D. Manogaran, S. Manogaran and H. F. I. Schaefer, *The Journal of Physical Chemistry A*, 2016, **120**, 2894–2901.

[9] S. Karashima, T. Ishiyama and T. Suzuki, *The Journal of Physical Chemistry Letters*, 2026, **17**, 410–416.

[10] L. L. Brunton, B. C. Knollmann, R. Hilal-Dandan *et al.*, *Goodman & Gilman's the pharmacological basis of therapeutics*, McGraw-Hill Education New York, 2018, vol. 13.

[11] S. B. Patil, *Heliyon*, 2023, **9**, e16773.

[12] B. Nammalwar and R. A. Bunce, *Pharmaceuticals*, 2024, **17**, 1–50.

[13] D. Diaconu, M. Savu, C. Ciobanu, V. Mangalagiu and I. I. Mangalagiu, *Bioorganic & Medicinal Chemistry*, 2025, **119**, 118069.

[14] G. A. Tsalidis, *Sustainability*, 2022, **14**, 1–12.

[15] R. A. Tucaliuc, V. Mangalagiu and I. I. Mangalagiu, *Processes*, 2023, **11**, 1–11.

[16] E. Saeedian Moghadam, F. Bonyasi, B. Bayati, M. Sadeghi Moghadam and M. Amini, *Journal of Agricultural and Food Chemistry*, 2024, **72**, 15427–15448.

[17] E. V. Verbitskiy, Y. A. Kvashnin, P. I. Bogdanov, M. V. Medvedeva, T. S. Svalova, A. N. Kozitsina, L. G. Samsonova, K. M. Degtyarenko, D. V. Grigoryev, A. E. Kurtcevich, R. M. Gadirov, G. L. Rusinov, O. N. Chupakhin and V. N. Charushin, *Dyes and Pigments*, 2021, **187**, 109124.

[18] S. Achelle, M. Hodée, J. Massue, A. Fihey and C. Katan, *Dyes and Pigments*, 2022, **200**, 110157.

[19] E. V. Verbitskiy, G. N. Lipunova, E. V. Nosova and V. N. Charushin, *Dyes and Pigments*, 2023, **220**, 111763.

[20] Q. Dun, L. Yao, Z. Deng, H. Li, J. Li, Y. Fan and B. Zhang, *LWT*, 2019, **112**, 107648.

[0d] *Department of Mathematics, School of Computation, Information and Technology, Technical University of Munich, Boltzmannstraße 3, 85748 Garching b. München; E-mail: antonia.freibert@tum.de*
[0b] *Department of Physics, University of Hamburg, Luruper Chaussee 149, 22761 Hamburg, Germany*
[0c] *Institute for Methods and Instrumentation for Synchrotron Radiation Research, Helmholtz-Zentrum Berlin für Materialien und Energie GmbH, 12489 Berlin, Germany*
[0d] *Institut für Physik und Astronomie, Universität Potsdam, 14476 Potsdam, Germany*

View Article Online
DOI: 10.1039/D6FD00063K

[21] A. Ren, Y. Zhang, Y. Bian, Y. jie Liu, Y. xin Zhang, C. jie Ren, Y. Zhou, T. Zhang and X. song Feng, *Food Chemistry*, 2024, **430**, 137086.

[22] M. Al-Khalili, P. B. Pathare, S. Rahman and N. Al-Habsi, *Measurement: Food*, 2025, **18**, 100220.

[23] M. Nuevo, C. K. Materese and S. A. Sandford, *The Astrophysical Journal*, 2014, **793**, 125.

[24] R. Borrego-Varillas, A. Nenov, P. Kabaciński, I. Conti, L. Ganzer, A. Oriana, V. K. Jaiswal, I. Delfino, O. Weingart, C. Manzoni, I. Rivalta, M. Garavelli and G. Cerullo, *Nature Communications*, 2021, **12**, 7285.

[25] Y. Miura, Y.-i. Yamamoto, S. Karashima, N. Orimo, A. Hara, K. Fukuoka, T. Ishiyama and T. Suzuki, *Journal of the American Chemical Society*, 2023, **145**, 3369–3381.

[26] P. Wu, X. Wang, H. Pan and J. Chen, *Journal of Photochemistry and Photobiology*, 2023, **18**, 100211.

[27] Y. Obara, S. Ghosh, A. Humeniuk, S. Kamibashira, S. Adachi and T. Suzuki, *Journal of the American Chemical Society*, 2025, **147**, 15077–15087.

[28] H. Bockholt, J. M. Beale and J. Rohr, *Angewandte Chemie International Edition in English*, 1994, **33**, 1648–1651.

[29] C. G. Wermuth, *Med. Chem. Commun.*, 2011, **2**, 935–941.

[30] Z.-X. He, Y.-P. Gong, X. Zhang, L.-Y. Ma and W. Zhao, *European Journal of Medicinal Chemistry*, 2021, **209**, 112946.

[31] N. A. Meanwell, *Medicinal Chemistry Research*, 2023, **32**, 1853–1921.

[32] G. Stock and W. Domcke, *J. Phys. Chem.*, 1993, **97**, 12466–12472.

[33] C. Woywod, W. Domcke, A. L. Sobolewski and H. Werner, *J. Chem. Phys.*, 1994, **100**, 1400–1413.

[34] A. Raab, G. A. Worth, H.-D. Meyer and L. S. Cederbaum, *J. Chem. Phys.*, 1999, **110**, 936–946.

[35] U. Werner, R. Mitrić, T. Suzuki and V. Bonačić-Koutecký, *Chem. Phys.*, 2008, **349**, 319–324.

[36] I. Burghardt, K. Giri and G. A. Worth, *J. Chem. Phys.*, 2008, **129**, 174104.

[37] D. V. Shalashilin, *J. Chem. Phys.*, 2010, **132**, 244111.

[38] M. Sala, B. Lasorne, F. Gatti and S. Guérin, *Phys. Chem. Chem. Phys.*, 2014, **16**, 15957–15967.

[39] M. Kanno, Y. Ito, N. Shimakura, S. Koseki, H. Kono and Y. Fujimura, *Phys. Chem. Chem. Phys.*, 2015, **17**, 2012–2024.

[40] T. Penfold, M. Pápai, K. Møller and G. Worth, *Comput. Theor. Chem.*, 2019, **1160**, 24–30.

[41] W. Xie, M. Sapunar, N. Došlić, M. Sala and W. Domcke, *J. Chem. Phys.*, 2019, **150**, 154119.

[42] M. F. Gelin, X. Huang, W. Xie, L. Chen, N. Došlić and W. Domcke, *J. Chem. Theory Comput.*, 2021, **17**, 2394–2408.

[43] T. Horio, R. Spesyvtsev, K. Nagashima, R. A. Ingle, Y.-i. Suzuki and T. Suzuki, *J. Chem. Phys.*, 2016, **145**, 044306.

[44] B. Mignolet, M. Kanno, N. Shimakura, S. Koseki, F. Remacle, H. Kono and Y. Fujimura, *Chem. Phys.*, 2018, **515**, 704–709.

[45] V. Scutelnic, S. Tsuru, M. Pápai, Z. Yang, M. Epshtein, T. Xue, E. Haugen, Y. Kobayashi, A. I. Krylov, K. B. Møller, S. Coriani and S. R. Leone, *Nat. Commun.*, 2021, **12**, 5003.

[46] T. Kaczun, A. L. Dempwolff, X. Huang, M. F. Gelin, W. Domcke and A. Dreuw, *J. Phys. Chem. Lett.*, 2023, **14**, 5648–5656.

[47] S. Karashima, A. Humeniuk and T. Suzuki, *Journal of the American Chemical Society*, 2024, **146**, 11067–11071.

[48] Y.-P. Chang, T. Balciunas, Z. Yin, M. Sapunar, B. N. C. Tenorio, A. C. Paul, S. Tsuru, H. Koch, J.-P. Wolf, S. Coriani and H. J. Wörner, *Nature Physics*, 2025, **21**, 137–145.

[49] L. J. Moore, M. J. Bearpark, G. A. Worth and M. A. Robb, *Chemical Physics*, 2026, **605**, 113115.

[50] P. Wernet, K. Kunnus, I. Josefsson, I. Rajkovic, W. Quevedo, M. Beye, S. Schreck, S. Grübel, M. Scholz, D. Nordlund, W. Zhang, R. W. Hartsock, W. F. Schlotter, J. J. Turner, B. Kennedy, F. Hennies, F. M. F. de Groot, K. J. Gaffney, S. Techert, M. Odelius and A. Föhlisch, *Nature*, 2015, **520**, 78–81.

[51] N. Ignatova, V. Kimberg, F. Gel'mukhanov, A. Pietzsch, S. Eckert, M. Fondell, B. Kennedy, M. Dantz, T. Schmitt, M. Odelius, A. Föhlisch and V. Vaz da Cruz, *Phys. Rev. A*, 2024, **110**, 033119.

View Article Online
DOI: 10.1039/D6FD00063K

[52] Y. Harada, T. Takeuchi, H. Kino, A. Fukushima, K. Takakura, K. Hieda, A. Nakao, S. Shin and H. Fukuyama, *The Journal of Physical Chemistry A*, 2006, **110**, 13227–13231.

[53] L. Weinhardt, E. Ertan, M. Iannuzzi, M. Weigand, O. Fuchs, M. Bär, M. Blum, J. D. Denlinger, W. Yang, E. Umbach, M. Odelius and C. Heske, *Phys. Chem. Chem. Phys.*, 2015, **17**, 27145–27153.

[54] A. Hussain, N. Huse and O. Vendrell, *Structural Dynamics*, 2017, **4**, 054102.

[55] V. Vaz da Cruz, F. Gel'mukhanov, S. Eckert, M. Iannuzzi, E. Ertan, A. Pietzsch, R. C. Couto, J. Niskanen, M. Fondell, M. Dantz, T. Schmitt, X. Lu, D. McNally, R. M. Jay, V. Kimberg, A. Föhlisch and M. Odelius, *Nature Communications*, 2019, **10**, 1013.

[56] Y. L. Jeyachandran, F. Meyer, S. Nagarajan, A. Benkert, M. Bär, M. Blum, W. Yang, F. Reinert, C. Heske, L. Weinhardt and M. Zharnikov, *The Journal of Physical Chemistry Letters*, 2014, **5**, 4143–4148.

[57] S. Eckert, J. Norell, P. S. Miedema, M. Beye, M. Fondell, W. Quevedo, B. Kennedy, M. Hantschmann, A. Pietzsch, B. E. Van Kuiken, M. Ross, M. P. Minitti, S. P. Moeller, W. F. Schlotter, M. Khalil, M. Odelius and A. Föhlisch, *Angewandte Chemie International Edition*, 2017, **56**, 6088–6092.

[58] V. Savchenko, I. E. Brumboiu, V. Kimberg, M. Odelius, P. Krasnov, J.-C. Liu, J.-E. Rubensson, O. Björneholm, C. Såthe, J. Gråsjö, M. Dong, A. Pietzsch, A. Föhlisch, T. Schmitt, D. McNally, X. Lu, S. P. Polyutov, P. Norman, M. Iannuzzi, F. Gel'mukhanov and V. Ekholm, *Scientific Reports*, 2021, **11**, 4098.

[59] V. Vaz da Cruz, R. Büchner, M. Fondell, A. Pietzsch, S. Eckert and A. Föhlisch, *The Journal of Physical Chemistry Letters*, 2022, **13**, 2459–2466.

[60] A. Nimmrich, N. Govind and M. Khalil, *The Journal of Physical Chemistry Letters*, 2024, **15**, 12652–12662.

[61] P. Wernet, K. Kunnus, S. Schreck, W. Quevedo, R. Kurian, S. Techert, F. M. F. de Groot, M. Odelius and A. Föhlisch, *The Journal of Physical Chemistry Letters*, 2012, **3**, 3448–3453.

[62] M. M. van Schooneveld, R. W. Gosselink, T. M. Eggenhuisen, M. Al Samarai, C. Monney, K. J. Zhou, T. Schmitt and F. M. F. de Groot, *Angewandte Chemie International Edition*, 2013, **52**, 1170–1174.

[63] A. W. Hahn, B. E. Van Kuiken, V. G. Chilkuri, N. Levin, E. Bill, T. Weyhermüller, A. Nicolaou, J. Miyawaki, Y. Harada and S. DeBeer, *Inorganic Chemistry*, 2018, **57**, 9515–9530.

[64] R. M. Jay, S. Eckert, M. Fondell, P. S. Miedema, J. Norell, A. Pietzsch, W. Quevedo, J. Niskanen, K. Kunnus and A. Föhlisch, *Phys. Chem. Chem. Phys.*, 2018, **20**, 27745–27751.

[65] R. M. Jay, S. Eckert, B. E. Van Kuiken, M. Ochmann, M. Hantschmann, A. A. Cordones, H. Cho, K. Hong, R. Ma, J. H. Lee, G. L. Dakovski, J. J. Turner, M. P. Minitti, W. Quevedo, A. Pietzsch, M. Beye, T. K. Kim, R. W. Schoenlein, P. Wernet, A. Föhlisch and N. Huse, *The Journal of Physical Chemistry Letters*, 2021, **12**, 6676–6683.

[66] E. Biasin, D. R. Nascimento, B. I. Poulter, B. Abraham, K. Kunnus, A. T. Garcia-Esparza, S. H. Nowak, T. Kroll, R. W. Schoenlein, R. Alonso-Mori, M. Khalil, N. Govind and D. Sokaras, *Chem. Sci.*, 2021, **12**, 3713–3725.

[67] T. Dederichs, A. Banerjee, V. Kabanova, R. Stefanuik, A. Freibert, E. V. Beale, F. Dworkowski, R. G. Castillo, P. J. M. Johnson, C. Cirelli, N. Huse, C. Bacellar, R. M. Jay and P. Wernet, *ChemRxiv*, 2025, **2025**,.

[68] R. M. Jay, A. Banerjee, M. Reinhard, H. Zhao, N. Huse, K. J. Gaffney, T. Kroll, D. Sokaras and P. Wernet, *Chem. Sci.*, 2026, –.

[69] F. Gel'mukhanov and H. Ågren, *Physics Reports*, 1999, **312**, 87–330.

[70] L. J. P. Ament, M. van Veenendaal, T. P. Devereaux, J. P. Hill and J. van den Brink, *Rev. Mod. Phys.*, 2011, **83**, 705–767.

[71] F. M. F. de Groot, M. W. Haverkort, H. Elnaggar, A. Juhin, K.-J. Zhou and P. Glatzel, *Nature Reviews Methods Primers*, 2024, **4**, 45.

[72] F. Gel'mukhanov and H. Ågren, *Phys. Rev. A*, 1994, **49**, 4378–4389.

[73] P. Skytt, J. Guo, N. Wassdahl, J. Nordgren, Y. Luo and H. Ågren, *Phys. Rev. A*, 1995, **52**, 3572–3576.

[74] Y.-P. Sun, A. Pietzsch, F. Hennies, Z. Rinkevicius, H. O. Karlsson, T. Schmitt, V. N. Strocov, J. Andersson, B. Kennedy, J. Schlappa, A. Föhlisch, F. Gel'mukhanov and J.-E. Rubensson, *Journal of Physics B: Atomic, Molecular and Optical Physics*, 2011, **44**, 161002.

[75] M. Ochmann, V. Vaz da Cruz, S. Eckert, N. Huse and A. Föhlisch, *Chem. Commun.*, 2022, **58**, 8834–8837.

[76] F. Gelmukhanov and H. Ågren, *Phys. Rev. A*, 1996, **54**, 379–393.

View Article Online
DOI: 10.1039/D5FD00063K

[77] O. Björneholm, S. Sundin, S. Svensson, R. R. T. Marinho, A. Naves de Brito, F. Gel'mukhanov and H. Ågren, *Phys. Rev. Lett.*, 1997, **79**, 3150–3153.

[78] S. Sundin, F. Kh. Gel'mukhanov, H. Ågren, S. J. Osborne, A. Kikas, O. Björneholm, A. Ausmees and S. Svensson, *Phys. Rev. Lett.*, 1997, **79**, 1451–1454.

[79] Y. Harada, T. Tokushima, Y. Takata, T. Takeuchi, Y. Kitajima, S. Tanaka, Y. Kayanuma and S. Shin, *Phys. Rev. Lett.*, 2004, **93**, 017401.

[80] F. Hennies, S. Polyutov, I. Minkov, A. Pietzsch, M. Nagasono, F. Gel'mukhanov, L. Triguero, M.-N. Piancastelli, W. Wurth, H. Ågren and A. Föhlisch, *Phys. Rev. Lett.*, 2005, **95**, 163002.

[81] D. Maganas, P. Kristiansen, L.-C. Duda, A. Knop-Gericke, S. DeBeer, R. Schlögl and F. Neese, *The Journal of Physical Chemistry C*, 2014, **118**, 20163–20175.

[82] S. Eckert, V. Vaz da Cruz, M. Ochmann, I. von Ahnen, A. Föhlisch and N. Huse, *The Journal of Physical Chemistry Letters*, 2021, **12**, 8637–8643.

[83] J. Schirmer, A. B. Trofimov, K. J. Randall, J. Feldhaus, A. M. Bradshaw, Y. Ma, C. T. Chen and F. Sette, *Phys. Rev. A*, 1993, **47**, 1136–1147.

[84] A. B. Trofimov, T. É. Moskovskaya, E. V. Gromov, N. M. Vitkovskaya and J. Schirmer, *Journal of Structural Chemistry*, 2000, **41**, 483–494.

[85] R. V. Pinjari, M. G. Delcey, M. Guo, M. Odelius and M. Lundberg, *The Journal of Chemical Physics*, 2014, **141**, 124116.

[86] J. Wenzel, M. Wormit and A. Dreuw, *Journal of Computational Chemistry*, 2014, **35**, 1900–1915.

[87] S. Coriani and H. Koch, *The Journal of Chemical Physics*, 2015, **143**, 181103.

[88] B. Peng, P. J. Lestrange, J. J. Goings, M. Caricato and X. Li, *Journal of Chemical Theory and Computation*, 2015, **11**, 4146–4153.

[89] D. R. Rehn, A. Dreuw and P. Norman, *Journal of Chemical Theory and Computation*, 2017, **13**, 5552–5559.

[90] M. L. Vidal, X. Feng, E. Epifanovsky, A. I. Krylov and S. Coriani, *Journal of Chemical Theory and Computation*, 2019, **15**, 3117–3133.

[91] M. L. Vidal, P. Pokhilko, A. I. Krylov and S. Coriani, *The Journal of Physical Chemistry Letters*, 2020, **11**, 8314–8321.

[92] B. Helmich-Paris, *International Journal of Quantum Chemistry*, 2021, **121**, e26559.

[93] W. Skomorowski, B. N. C. Tenorio and S. Coriani, *Phys. Chem. Chem. Phys.*, 2025, **27**, 20117–20130.

[94] N. A. Besley and F. A. Asmuruf, *Phys. Chem. Chem. Phys.*, 2010, **12**, 12024–12039.

[95] N. A. Besley, *Accounts of Chemical Research*, 2020, **53**, 1306–1315.

[96] N. A. Besley, *WIREs Computational Molecular Science*, 2021, **11**, e1527.

[97] P. Norman and A. Dreuw, *Chemical Reviews*, 2018, **118**, 7208–7248.

[98] Z. Mathe, D. Maganas, F. Neese and S. DeBeer, *Nature Reviews Chemistry*, 2025, **9**, 436–453.

[99] F. Gel'mukhanov, M. Odelius, S. P. Polyutov, A. Föhlisch and V. Kimberg, *Rev. Mod. Phys.*, 2021, **93**, 035001.

[100] E. Muchova, D. Hollas, D. M. P. Holland, C. Bacellar, L. Leroy, T. R. Barillot, L. Longetti, M. Coreno, M. de Simone, C. Grazioli, M. Chergui and R. A. Ingle, *Phys. Chem. Chem. Phys.*, 2023, **25**, 6733–6745.

[101] F. Gel'mukhanov, J.-C. Liu, P. Krasnov, N. Ignatova, J.-E. Rubensson and V. Kimberg, *Phys. Rev. A*, 2023, **108**, 052820.

[102] J. Söderström, A. Ghosh, L. Kjellsson, V. Ekholm, T. Tokushima, C. Såthe, N. Velasquez, M. Simon, O. Björneholm, L. Duda, A. N. de Brito, M. Odelius, J.-C. Liu, J. Wang, V. Kimberg, M. Agåker, J.-E. Rubensson and F. Gel'mukhanov, *Science Advances*, 2024, **10**, eadk3114.

[103] D. M. P. Holland, J. Suchan, J. Janoš, C. Bacellar, L. Leroy, T. R. Barillot, L. Longetti, M. Coreno, M. de Simone, C. Grazioli, M. Chergui, E. Muchová and R. A. Ingle, *Phys. Chem. Chem. Phys.*, 2024, **26**, 15130–15142.

[104] D. M. P. Holland, H. G. McGhee, M. Lamanec, D. Nachtigallová, A. Milosavljević, J. D. Bozek, E. Muchová and R. A. Ingle, *Chem. Sci.*, 2026, –.

[105] D. Maganas, S. DeBeer and F. Neese, *Inorganic Chemistry*, 2017, **56**, 11819–11836.

View Article Online
DOI: 10.1039/D6FD00063K

[106] E. Vitols, V. Vaz da Cruz, T. Fransson and I. E. Brumboiu, *The Journal of Physical Chemistry A*, 2025, **129**, 8783–8797.

[107] V. Vaz da Cruz, S. Eckert and A. Föhlisch, *Phys. Chem. Chem. Phys.*, 2021, **23**, 1835–1848.

[108] M. P. Ljungberg, *Phys. Rev. B*, 2017, **96**, 214302.

[109] N. Ignatova, V. V. Cruz, R. C. Couto, E. Ertan, A. Zimin, F. F. Guimarães, S. Polyutov, H. Ågren, V. Kimberg, M. Odelius and F. Gel'mukhanov, *Scientific Reports*, 2017, **7**, 43891.

[110] R. C. Couto, V. V. Cruz, E. Ertan, S. Eckert, M. Fondell, M. Dantz, B. Kennedy, T. Schmitt, A. Pietzsch, F. F. Guimarães, H. Ågren, F. Gel'mukhanov, M. Odelius, V. Kimberg and A. Föhlisch, *Nature Communications*, 2017, **8**, 14165.

[111] V. Vaz da Cruz, E. Ertan, R. C. Couto, S. Eckert, M. Fondell, M. Dantz, B. Kennedy, T. Schmitt, A. Pietzsch, F. F. Guimarães, H. Ågren, F. Gel'mukhanov, M. Odelius, A. Föhlisch and V. Kimberg, *Phys. Chem. Chem. Phys.*, 2017, **19**, 19573–19589.

[112] R. C. Couto, M. Guarise, A. Nicolaou, N. Jaouen, G. S. Chiuzbăian, J. Lüning, V. Ekholm, J.-E. Rubensson, C. Såthe, F. Hennies, F. F. Guimarães, H. Ågren, F. Gel'mukhanov, L. Journel, M. Simon and V. Kimberg, *Phys. Rev. A*, 2016, **93**, 032510.

[113] A. Freibert, D. Mendive-Tapia, N. Huse and O. Vendrell, *Journal of Chemical Theory and Computation*, 2024, **20**, 2167–2180.

[114] H.-D. Meyer, U. Manthe and L. Cederbaum, *Chemical Physics Letters*, 1990, **165**, 73–78.

[115] M. Ohno, *J. Electron Spectrosc. Relat. Phenom.*, 2005, **143**, 13–19.

[116] C. Nicolas and C. Miron, *J. Electron Spectrosc. Relat. Phenom.*, 2012, **185**, 267–272.

[117] P. A. M. Dirac, *Proc. R. Soc. Lond. A Math. Phys. Sci.*, 1927, **114**, 243–265.

[118] R. Schinke, *Photodissociation Dynamics: Spectroscopy and Fragmentation of Small Polyatomic Molecules*, Cambridge University Press, 1995.

[119] H. A. Kramers and W. Heisenberg, *Zeitschrift für Physik*, 1925, **31**, 681–708.

[120] P. Dirac and R. Fowler, *Proc. R. Soc. Lond. A Math. Phys. Sci.*, 1927, **114**, 710–728.

[121] D. J. Tannor and E. J. Heller, *J. Chem. Phys.*, 1982, **77**, 202–218.

[122] U. Manthe, H. Meyer and L. S. Cederbaum, *J. Chem. Phys.*, 1992, **97**, 3199–3213.

[123] M. Beck, A. Jäckle, G. Worth and H.-D. Meyer, *Phys. Rep.*, 2000, **324**, 1–105.

[124] H. Wang and M. Thoss, *J. Chem. Phys.*, 2003, **119**, 1289–1299.

[125] U. Manthe, *J. Chem. Phys.*, 2008, **128**, 164116.

[126] O. Vendrell and H.-D. Meyer, *J. Chem. Phys.*, 2011, **134**, 044135.

[127] H. Wang, *J. Phys. Chem. A*, 2015, **119**, 7951–7965.

[128] G. A. Worth, H.-D. Meyer, H. Köppel, L. S. Cederbaum and I. Burghardt, *Int. Rev. Phys. Chem.*, 2008, **27**, 569–606.

[129] H.-D. Meyer, F. Gatti and G. A. Worth, *Multidimensional Quantum Dynamics*, John Wiley & Sons, Ltd, 2009.

[130] A. Freibert, D. Mendive-Tapia, N. Huse and O. Vendrell, *Journal of Physics B: Atomic, Molecular and Optical Physics*, 2022, **54**, 244003.

[131] A. Freibert, D. Mendive-Tapia, O. Vendrell and N. Huse, *Phys. Chem. Chem. Phys.*, 2024, **26**, 22572–22581.

[132] L. Cederbaum, W. Domcke, H. Köppel and W. Von Niessen, *Chem. Phys.*, 1977, **26**, 169–177.

[133] W. Domcke and L. Cederbaum, *Chem. Phys.*, 1977, **25**, 189–196.

[134] H. Köuppel, W. Domcke and L. S. Cederbaum, in *Multimode Molecular Dynamics Beyond the Born-Oppenheimer Approximation*, John Wiley & Sons, Ltd, 1984, pp. 59–246.

[135] L. S. Cederbaum and W. Domcke, *The Journal of Chemical Physics*, 1977, **66**, 5084–5086.

[136] L. S. Cederbaum, *The Journal of Chemical Physics*, 1995, **103**, 562–567.

[137] N. Kosugi, *Chem. Phys.*, 2003, **289**, 117–134.

[138] P. S. Bagus and I. Schaefer, Henry F., *J. Chem. Phys.*, 2003, **56**, 224–226.

View Article Online
DOI: 10.1039/D6FD00063K

[139] A. Pietzsch and S. Eisebitt, *J. Large-scale Res. Facil. JLSRF*, 2016, **2**, year.

[140] K. Kunnus, I. Rajkovic, S. Schreck, W. Quevedo, S. Eckert, M. Beye, E. Suljoti, C. Weniger, C. Kalus, S. Grübel, M. Scholz, D. Nordlund, W. Zhang, R. W. Hartsock, K. J. Gaffney, W. F. Schlotter, J. J. Turner, B. Kennedy, F. Hennies, S. Techert, P. Wernet and A. Föhlisch, *The Review of Scientific Instruments*, 2012, **83**, 123109.

[141] M. Fondell, S. Eckert, R. M. Jay, C. Weniger, W. Quevedo, J. Niskanen, B. Kennedy, F. Sorgenfrei, D. Schick, E. Giangrisostomi, R. Ovsyannikov, K. Adamczyk, N. Huse, P. Wernet, R. Mitzner and A. Föhlisch, *Structural Dynamics*, 2017, **4**, 054902.

[142] C. Møller and M. S. Plesset, *Phys. Rev.*, 1934, **46**, 618–622.

[143] T. H. Dunning, *The Journal of Chemical Physics*, 1989, **90**, 1007–1023.

[144] M. J. Frisch, G. W. Trucks, H. B. Schlegel, G. E. Scuseria, M. A. Robb, J. R. Cheeseman, G. Scalmani, V. Barone, G. A. Petersson, H. Nakatsuji, X. Li, M. Caricato, A. V. Marenich, J. Bloino, B. G. Janesko, R. Gomperts, B. Mennucci, H. P. Hratchian, J. V. Ortiz, A. F. Izmaylov, J. L. Sonnenberg, D. Williams-Young, F. Ding, F. Lipparini, F. Egidi, J. Goings, B. Peng, A. Petrone, T. Henderson, D. Ranasinghe, V. G. Zakrzewski, J. Gao, N. Rega, G. Zheng, W. Liang, M. Hada, M. Ehara, K. Toyota, R. Fukuda, J. Hasegawa, M. Ishida, T. Nakajima, Y. Honda, O. Kitao, H. Nakai, T. Vreven, K. Throssell, J. A. Montgomery, Jr., J. E. Peralta, F. Ogliaro, M. J. Bearpark, J. J. Heyd, E. N. Brothers, K. N. Kudin, V. N. Staroverov, T. A. Keith, R. Kobayashi, J. Normand, K. Raghavachari, A. P. Rendell, J. C. Burant, S. S. Iyengar, J. Tomasi, M. Cossi, J. M. Millam, M. Klene, C. Adamo, R. Cammi, J. W. Ochterski, R. L. Martin, K. Morokuma, O. Farkas, J. B. Foresman and D. J. Fox, *Gaussian 16 Revision A.03*, 2016, Gaussian Inc. Wallingford CT.

[145] J. F. Stanton and R. J. Bartlett, *The Journal of Chemical Physics*, 1993, **98**, 7029–7039.

[146] E. Epifanovsky, A. T. B. Gilbert, X. Feng, J. Lee, Y. Mao, N. Mardirossian, P. Pokhilko, A. F. White, M. P. Coons, A. L. Dempwolff, Z. Gan, D. Hait, P. R. Horn, L. D. Jacobson, I. Kaliman, J. Kussmann, A. W. Lange, K. U. Lao, D. S. Levine, J. Liu, S. C. McKenzie, A. F. Morrison, K. D. Nanda, F. Plasser, D. R. Rehn, M. L. Vidal, Z.-Q. You, Y. Zhu, B. Alam, B. J. Albrecht, A. Aldossary, E. Alguire, J. H. Andersen, V. Athavale, D. Barton, K. Begam, A. Behn, N. Bellonzi, Y. A. Bernard, E. J. Berquist, H. G. A. Burton, A. Carreras, K. Carter-Fenk, R. Chakraborty, A. D. Chien, K. D. Closser, V. Cofer-Shabica, S. Dasgupta, M. de Wergifosse, J. Deng, M. Diedenhofen, H. Do, S. Ehlert, P.-T. Fang, S. Fatehi, Q. Feng, T. Friedhoff, J. Gayvert, Q. Ge, G. Gidofalvi, M. Goldey, J. Gomes, C. E. González-Espinoza, S. Gulania, A. O. Gunina, M. W. D. Hanson-Heine, P. H. P. Harbach, A. Hauser, M. F. Herbst, M. Hernández Vera, M. Hodecker, Z. C. Holden, S. Houck, X. Huang, K. Hui, B. C. Huynh, M. Ivanov, A. Jász, H. Ji, H. Jiang, B. Kaduk, S. Kähler, K. Khistyaev, J. Kim, G. Kis, P. Klunzinger, Z. Koczor-Benda, J. H. Koh, D. Kosenkov, L. Koulias, T. Kowalczyk, C. M. Krauter, K. Kue, A. Kunitsa, T. Kus, I. Ladjánszki, A. Landau, K. V. Lawler, D. Lefrancois, S. Lehtola, R. R. Li, Y.-P. Li, J. Liang, M. Liebenthal, H.-H. Lin, Y.-S. Lin, F. Liu, K.-Y. Liu, M. Loipersberger, A. Luenser, A. Manjanath, P. Manohar, E. Mansoor, S. F. Manzer, S.-P. Mao, A. V. Marenich, T. Markovich, S. Mason, S. A. Maurer, P. F. McLaughlin, M. F. S. J. Menger, J.-M. Mewes, S. A. Mewes, P. Morgante, J. W. Mullinax, K. J. Oosterbaan, G. Paran, A. C. Paul, S. K. Paul, F. Pavošević, Z. Pei, S. Prager, E. I. Proynov, A. Rak, E. Ramos-Cordoba, B. Rana, A. E. Rask, A. Rettig, R. M. Richard, F. Rob, E. Rossomme, T. Scheele, M. Scheurer, M. Schneider, N. Sergueev, S. M. Sharada, W. Skomorowski, D. W. Small, C. J. Stein, Y.-C. Su, E. J. Sundstrom, Z. Tao, J. Thirman, G. J. Tornai, T. Tsuchimochi, N. M. Tubman, S. P. Veccham, O. Vydrov, J. Wenzel, J. Witte, A. Yamada, K. Yao, S. Yeganeh, S. R. Yost, A. Zech, I. Y. Zhang, X. Zhang, Y. Zhang, D. Zuev, A. Aspuru-Guzik, A. T. Bell, N. A. Besley, K. B. Bravaya, B. R. Brooks, D. Casanova, J.-D. Chai, S. Coriani, C. J. Cramer, G. Cserey, I. DePrince, A. Eugene, J. DiStasio, Robert A., A. Dreuw, B. D. Dunietz, T. R. Furlani, I. Goddard, William A., S. Hammes-Schiffer, T. Head-Gordon, W. J. Hehre, C.-P. Hsu, T.-C. Jagau, Y. Jung, A. Klamt, J. Kong, D. S. Lambrecht, W. Liang, N. J. Mayhall, C. W. McCurdy, J. B. Neaton, C. Ochsenfeld, J. A. Parkhill, R. Peverati, V. A. Rassolov, Y. Shao, L. V. Slipchenko, T. Stauch, R. P. Steele, J. E. Subotnik, A. J. W. Thom, A. Tkatchenko, D. G. Truhlar, T. Van Voorhis, T. A. Wesolowski, K. B. Whaley, I. Woodcock, H. Lee, P. M. Zimmerman, S. Faraji, P. M. W. Gill, M. Head-Gordon, J. M. Herbert and A. I. Krylov, *The Journal of Chemical Physics*, 2021, **155**, 084801.

[147] G. A. Worth, M. H. Beck, A. Jäckle, H. Meyer, F. Otto, M. Brill and O. Vendrell, *The MCTDH package, version 8.6*, 2020, `http://mctdh.uni-hd.de`.

[148] K. Prince, M. Vondráček, J. Karvonen, M. Coreno, R. Camilloni, L. Avaldi and M. de Simone, *J. Electron Spectrosc. Relat. Phenom.*, 1999, **101-103**, 141–147.

[149] J. O. Edwards and R. G. Pearson, *Journal of the American Chemical Society*, 1962, **84**, 16–24.

[150] E. J. Heller, R. Sundberg and D. Tannor, *J. Phys. Chem.*, 1982, **86**, 1822–1833.

View Article Online
DOI: 10.1039/D6FD00063K

Data availability

The data supporting this article have been included as part of the Supplementary Information.